

Effects of Aluminum Over-layer Thickness on Characteristics of Niobium Tunnel Junctions Fabricated by DC Magnetron Sputtering

Akiyoshi Nakayama, Haruo Nagashima, Jun'ichi Shimada
Department of Electrical Engineering, Faculty of Engineering, Kanagawa University
3-27-1, Rokkakubashi, Kanagawa-ku, Yokohama, 221, Japan

Yoichi Okabe
Research Center for Advanced Science and Technology, University of Tokyo
4-6-1, Komaba, Meguro-ku, Tokyo, 153, Japan

Abstract—We have fabricated Nb/AlO_x/Nb Josephson tunnel junctions using a sputtering apparatus with a load-lock system. The junctions that had 50 μm × 50 μm area showed a V_m value (the product of the critical current and the subgap resistance at 2 mV) as high as 50 mV at a current density of 160 A/cm². Moreover, junctions having different thicknesses of the Al over-layer were concurrently fabricated on one wafer to study the dependence of the current-voltage characteristics on this Al over-layer. The I-V characteristics were also calculated by McMillan's tunneling model and were compared with the measured I-V characteristics.

I. INTRODUCTION

Niobium Josephson tunnel junctions are potentially very useful in the realization of high-speed, low-power integrated circuits for many electronic applications, e. g. digital and analog circuits and sensitive magnetic sensors. Its excellent electrical characteristics, durability and thermal cyclability make it a promising device for application of superconductivity [1]. Niobium/aluminum-oxide/niobium (Nb/AlO_x/Nb) Josephson tunnel junctions have been fabricated by electron-beam deposition [2, 3] or magnetron sputtering [4, 5]. In order to obtain Nb films with good superconducting properties by sputtering, Nb has to be deposited in very pure Ar gas, because niobium easily reacts with oxygen and degrades its superconducting properties. In a sputtering system, we can not measure the exact background pressure during the sputtering. Hence, both a background pressure better than 10⁻⁵ Pa and low outgassing from the chamber wall are needed for a sputtering system to fabricate Nb/AlO_x/Nb junctions.

This paper reports the fabrication of Nb/AlO_x/Nb Josephson tunnel junctions by a sputtering apparatus with load-lock system. In sect. II, the sputtering system and the fabrication process of the Nb junctions are mentioned. Fabrication technique for varying the thickness of the Al over-layer is also presented. In sect. III.A, current-voltage characteristics of the Nb/AlO_x/Nb junctions at 4.2 K are mentioned. In sect. III.B, the characteristics of the junctions with different Al thicknesses are studied. In sect. III.C,

the I-V characteristics of the Nb junctions calculated with McMillan's tunneling model are mentioned. We obtained the density of states (DOS) of the electrodes of the Nb junctions by this model and calculated the tunneling current to obtain the current-voltage characteristics and to compare them with the measured I-V characteristics. Section IV presents our conclusions.

II. FABRICATION

Niobium/aluminum-oxide/niobium Josephson tunnel junctions were fabricated by a vacuum system with a load-lock chamber. This system consisted of four parts: a sputtering main chamber, a sputtering sub chamber, a chamber for oxidation, and a preparation chamber. The sputtering main chamber had sputtering guns for Nb and Al depositions, and was always maintained as low as 10⁻⁶ Pa range by a 60 l/s triode ion pump, an 800 l/s Ti sublimation pump and a 1600 l/s cryo pump. Nb and Al films were deposited by DC magnetron sputtering.

The preparation chamber was used for a first entry lock chamber. Since the volume of the preparation chamber was as small as 1 liter, a 200 l/s turbo-molecular pump evacuated this chamber from the atmosphere to the 10⁻⁵ Pa range within 30 minutes. Hence, this sputtering apparatus with the load lock system shortened the fabrication time of Nb/AlO_x/Nb junctions.

In the sputtering sub chamber, there is another sputtering gun for Al deposition. Many junctions that had different Al thicknesses were simultaneously fabricated. By moving the shutter 4 mm above the substrate during the deposition of Al film, we could fabricate the junctions having the different Al thicknesses on 2-inch Si wafer substrate. The size of the shutter was 5 cm × 3 cm and was also made of Si wafer. The shutter was moved as much as 50 mm by linear motion drive. The precision of the movement was 10 μm.

The fabrication process of the Nb junctions was as follows: After Nb base electrode was deposited on the substrate in the sputtering main chamber, the Al over-layer was deposited by sputtering in the sputtering sub chamber. The substrate was moved from one chamber to another by magnetic-coupled linear motion drives. The surface of the Al over-layer was then oxidized in the preparation chamber by introducing pure oxygen. Oxidation was done in 2.7 × 10³ Pa oxygen for 30 minutes without heating the substrate. After the Nb counter-

Manuscript received in October 18, 1994.

electrode was deposited in the main chamber, the junction areas of the Nb/AlO_x/Nb tri-layers were defined by selective niobium anodization process. Finally, the wiring Nb electrode was deposited and was patterned by chemical etching.

III. RESULTS AND DISCUSSIONS

A. I-V characteristics

Figure 1 shows the current-voltage characteristics of the fabricated Nb/AlO_x/Nb tunnel junction at 4.2 K. The V_m value (the product of the critical current and the subgap resistance at 2 mV) of this junction was as high as 50 mV. The junction size was 50 $\mu\text{m} \times 50 \mu\text{m}$. The V_m value of a 10 $\mu\text{m} \times 10 \mu\text{m}$ junction and that of a 5 $\mu\text{m} \times 5 \mu\text{m}$ junction were 33 mV and 31 mV, respectively.

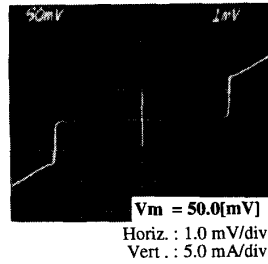


Fig. 1. Current-voltage characteristics of the Nb/AlO_x/Nb junction at 4.2 K. The junction area was 50 $\mu\text{m} \times 50 \mu\text{m}$.

B. Dependence on the Al over-layer thickness

We studied the dependence of the junctions' I-V characteristics upon the thickness of the Al over-layer. Lots of junctions having different Al thicknesses were concurrently fabricated on one Si wafer by moving the shutter during the deposition of Al over-layer. By fabricating the junctions on the same wafer, we can obtain the junctions having the same process conditions other than the thicknesses of the Al over-layer. Figure 2 shows the dependence of the Nb/AlO_x/Nb junctions' characteristics upon the thickness of the Al over-layer deposited on the Nb base electrode. Several junctions that lay in the perpendicular direction to the shutter's movement, had the same Al thickness. The values of the characteristics of these junctions with the same Al thickness had however a little spread as shown in this figure, probably because the Al layer was not perfectly uniform in the perpendicular direction to the shutter's movement.

When the Al thickness was less than 2 nm, the R_{sg}/R_n ratio and the V_m value became low. It is possibly because the coverage of the Al over-layer was poor and the tunnel barrier could not be formed uniformly. When the Al layer became thicker than 4 nm the characteristics also became poor, because the proximity layer between the base electrode and

the tunnel oxide became thicker. The best I-V characteristics were obtained when the Al thickness was 3 nm.

C. Calculation of I-V characteristics by McMillan's Tunneling Model

We have calculated the current-voltage characteristics of the Nb tunnel junctions by McMillan's Tunneling Model (MTM) [6]. We consider that the Nb/AlO_x/Nb junctions have a structure of superconductor/proximity-layer/barrier/proximity-layer/superconductor, where the proximity layer of the base electrode is Al over-layer. We also think that there is an inter-diffusion layer between the AlO_x and the Nb counter-electrode as the proximity layer of the counter-electrode side. The density of states of the proximity layer (normal layer) and that of the superconducting layer are obtained from the equations:

$$N_N(E) = \text{Re} \left\{ E \left[E^2 - \Delta_N^2(E) \right]^{1/2} \right\}, \quad (1)$$

$$N_S(E) = \text{Re} \left\{ E \left[E^2 - \Delta_S^2(E) \right]^{1/2} \right\}, \quad (2)$$

where the $\Delta_N(E)$ and $\Delta_S(E)$ are obtained by the numerical calculation of the equations as follows:

$$\Delta_N(E) = \left(\Delta_N^{ph} + \frac{\Gamma_N \Delta_S(E)}{[\Delta_S^2(E) - E^2]^{1/2}} \right) \left(1 + \frac{\Gamma_N}{[\Delta_S^2(E) - E^2]^{1/2}} \right), \quad (3)$$

$$\Delta_S(E) = \left(\Delta_S^{ph} + \frac{\Gamma_S \Delta_N(E)}{[\Delta_N^2(E) - E^2]^{1/2}} \right) \left(1 + \frac{\Gamma_S}{[\Delta_N^2(E) - E^2]^{1/2}} \right). \quad (4)$$

Figure 3 shows the I-V characteristics calculated using MTM. The lifetime broadening parameters Γ_N and Γ_S , and the fixed BCS potentials Δ_N^{ph} and Δ_S^{ph} assumed in the numerical calculation with MTM are mentioned in the figure captions in Fig. 3. The lifetime broadening parameters Γ_N and Γ_S are inversely proportional to the thickness of the proximity layer and that of the superconducting layer, respectively. Current-voltage curve with the different Γ_N and Γ_S parameters are showed in the figure, where the subscripts [1] and [2] represent the base electrode and the counter-electrode, respectively. $\Gamma_N = 0.025$ eV and $\Gamma_N = 0.25$ eV are correspondent with the 4.0 nm and 0.4 nm proximity layer, respectively, and $\Gamma_S = 3.9 \times 10^{-5}$ eV with 200 nm superconducting layer. The gap voltage becomes small and the sub-gap leak-current becomes large when the thickness of the proximity layer becomes thicker. The I-V curve doesn't strongly depend on the thickness of the superconducting layer as shown in Fig. 3(c). Temperature dependence of the I-V curve is also obtained as shown in Fig. 3(d). Comparing with the measured I-V curve, the thicknesses of the proximity layers of the base and the counter-electrode are estimated to be 4.0 nm and 0.4 nm, respectively.

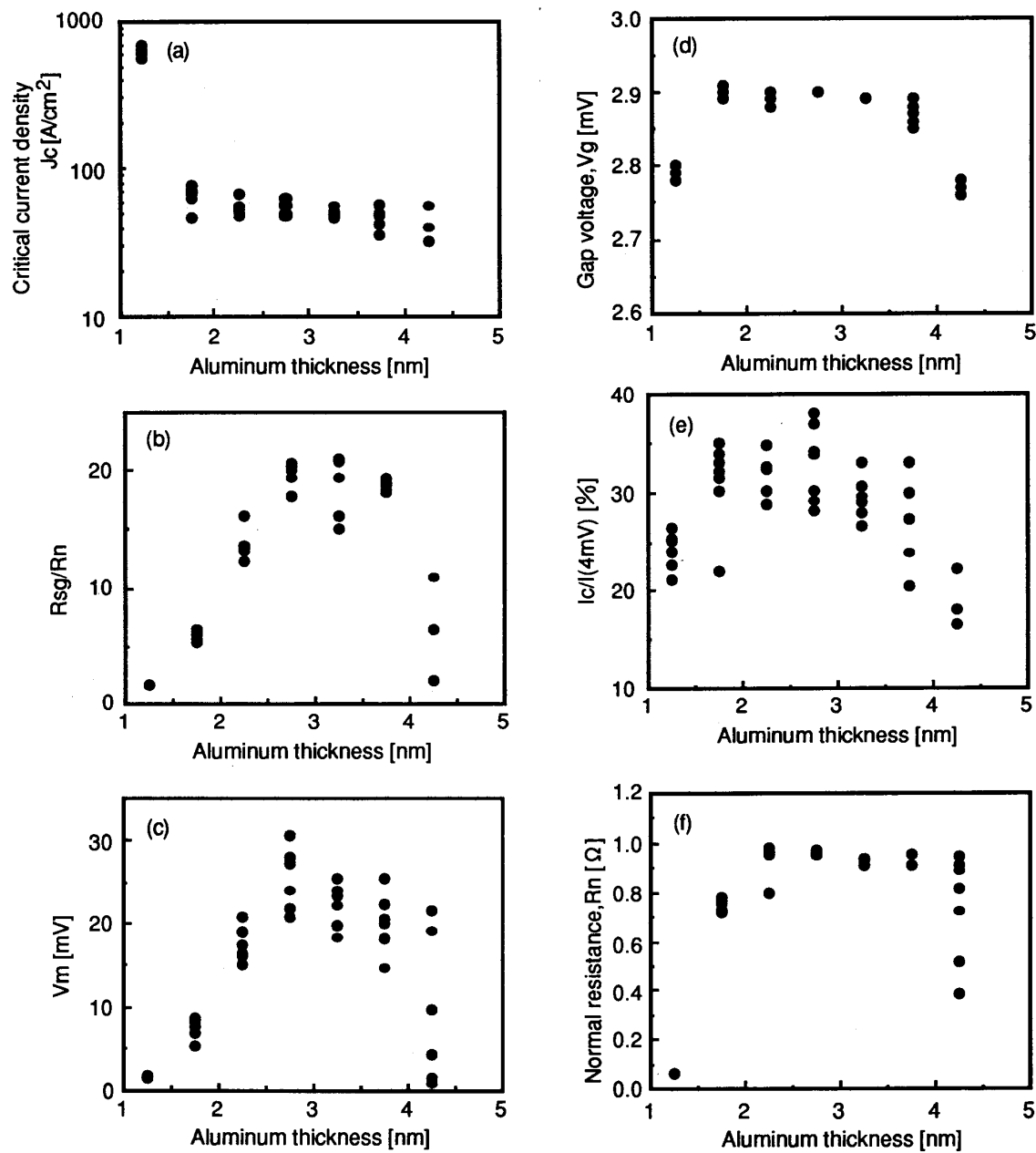


Fig. 2. Dependence of the I-V characteristics upon the thickness of the Al over-layer. Dependence of (a) critical current density, J_c , (b) R_{sg}/R_n , (c) V_m , (d) gap voltage, V_g , (e) $I_c/I(4\text{ mV})$, and (f) normal resistance R_n of the I-V characteristics of the Nb/ AlO_x /Nb junctions at 4.2 K is shown, where the subgap resistance R_{sg} and the normal resistance R_n are measured at 2 mV and at 4 mV, respectively, and $I(4\text{ mV})$ is the current value at 4 mV. The junction areas are $50\text{ }\mu\text{m} \times 50\text{ }\mu\text{m}$.

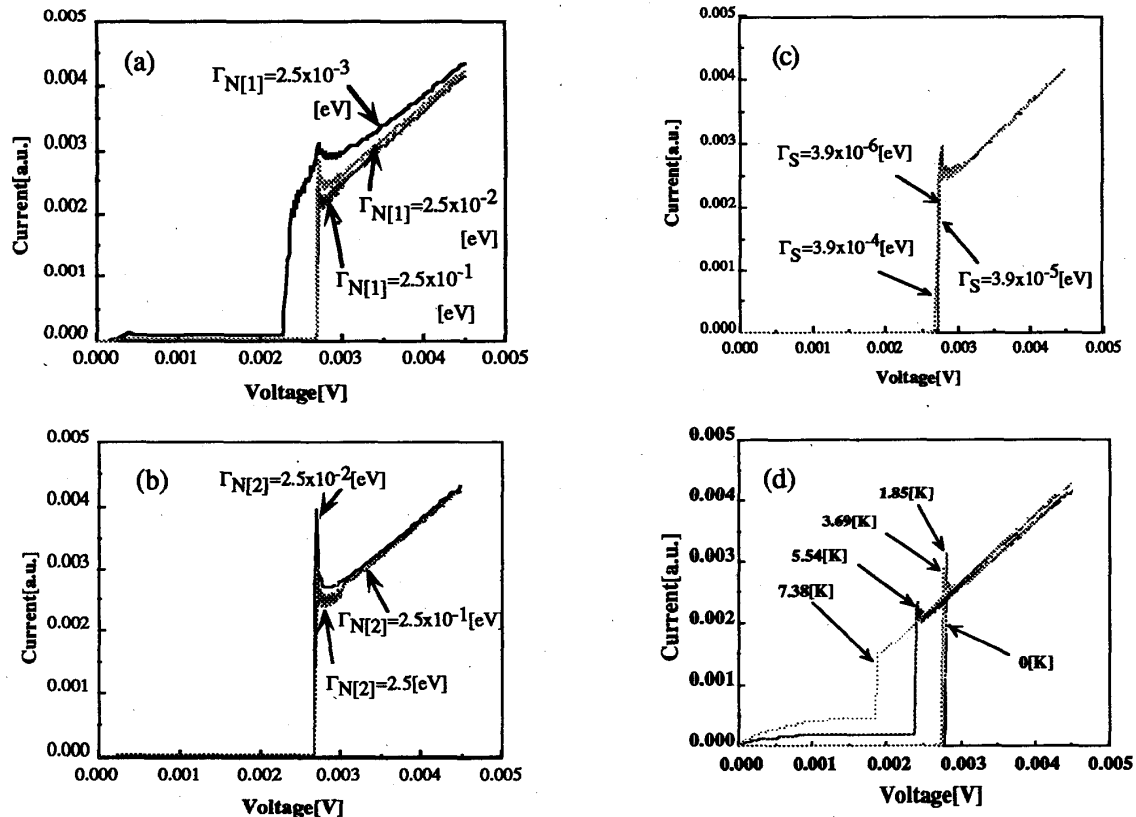


Fig. 3. Current-voltage characteristics calculated by McMillan's tunneling model. The critical temperature of superconducting layer (T_c) and that of normal layer are 9.23 K and 1.196 K, respectively. $\Delta_s^{\text{ph}} = 1.38 \times 10^{-3}$ eV, $\Delta_N^{\text{ph}} = 1.38 \times 10^{-4}$ eV. (a) dependence on $\Gamma_{N[1]}$ ($\Gamma_s = 3.9 \times 10^{-5}$ eV, $\Gamma_{N[2]} = 2.5 \times 10^{-4}$ eV, $T = 0.4 T_c$), (b) dependence on $\Gamma_{N[2]}$ ($\Gamma_s = 3.9 \times 10^{-5}$ eV, $\Gamma_{N[1]} = 2.5 \times 10^{-2}$ eV, $T = 0.4 T_c$), (c) dependence on Γ_s ($\Gamma_{N[1]} = 2.5 \times 10^{-2}$ eV, $\Gamma_{N[2]} = 2.5 \times 10^{-1}$ eV, $T = 0.4 T_c$), (d) temperature dependence of I-V characteristics ($\Gamma_s = 3.9 \times 10^{-5}$ eV, $\Gamma_{N[1]} = 2.5 \times 10^{-2}$ eV, $\Gamma_{N[2]} = 2.5 \times 10^{-1}$ eV, $T = 0, 0.2 T_c, 0.4 T_c, 0.6 T_c, 0.8 T_c$).

IV. CONCLUSIONS

In summary, the characteristics of the Nb/AlO_x/Nb Josephson tunnel junctions fabricated by a sputtering apparatus with a load-lock system have been presented. The sputtering apparatus had two chambers for sputtering, a sub chamber for oxidation and a sub chamber for preparation. The junctions that had $50 \mu\text{m} \times 50 \mu\text{m}$ area successfully showed the V_m value as high as 50 mV at the current density of 160 A/cm². Moreover, junctions having different thicknesses of the Al over-layer were concurrently fabricated on one wafer in order to study the dependence of the I-V characteristics upon the thickness of the Al over-layer. The I-V characteristics were also calculated by McMillan's tunneling model and were compared with the measured I-V characteristics.

REFERENCES

[1] Hasuo, S., Kotani, S., Inoue, A. and Fujimaki, N., "High

- Speed Josephson Processor Technology," *Trans. on Mag.*, vol. MAG-27, no. 2, pp. 2602-2609, Mar. 1991.
- [2] Broom, R. F., Laibowitz, R. B., Mohr, Th. O. and Walter, W., "Fabrication and Properties of Niobium Josephson Tunnel Junctions," *IBM J. Res. Develop.*, vol. 24, no. 2, Mar. 1980.
- [3] Inoue, A., Nakayama, A. and Okabe, Y., "Nb/AlO_x/Nb Josephson Tunnel Junctions Using Electron Beam Evaporation," *Jpn. J. Appl. Phys.* vol. 27, no. 7, pp. 1234-1239, Jul. 1988.
- [4] Gurvitch, M., Washington, M. A. and Huggins, H. A., "High Quality Refractory Josephson tunnel junctions utilizing thin aluminum layers," *Appl. Phys. Lett.*, vol. 42, no. 5, pp. 472-474, Mar. 1983.
- [5] Morohashi, S., Shinoki, F., Shoji, M. and Hayakawa, H., "High quality Nb/Al-AlO_x/Nb Josephson junctions," *Appl. Phys. Lett.*, vol. 46, no. 12, pp. 1179-1181, Jun. 1985.
- [6] W.L. McMillan, "Tunneling Model of the Superconducting Proximity Effect," *Phys. Rev.*, vol. 175, no. 2, pp. 537-542, Nov. 1968.